Study of Corrosion Resistant Property of Benzoxazine Synthesised from Euginol with n-butylamine and Copolymerised with Polyurethane on mild steel

JAYANTHI KANNAIYAN[1]* and SIVARAJU MANI[2]

[1]*Department of Chemistry, Queen Mary's College(A), Chennai–Pincode 600004, Tamil Nadu, India.
[2]Department of Chemistry, Thiruvalluvar Government Arts College, Rasipuram, Pincode 637401, Tamil Nadu, India.
*Corresponding author E-mail: kjayanthi_che@queenmaryscollege.edu.in

ABSTRACT

In this work, we have synthesized a new eugenol based benzoxazine monomer from eugenol, paraformaldehyde and n-butyl amine. The synthesized monomer was characterized by ^{1}H NMR, ^{13}C NMR, UV-Visible and FT-IR spectroscopy. The monomer was then co-polymerized with isocyanate hardener on the surface of the mild steel with three different composition. After that it was cured in a muffle furnace to get poly(benzoxazine-urethane). The copolymer's characterized by UV and FT-IR spectroscopic techniques. The anti-corrosive property of the co-polymer was investigated using polarization and EIS techniques against 3.5% NaCl solution. For additional support for this work, DFT studies also carried out for monomer and its copolymer. Water absorption and gel absorption studies were also done to add evidences for the hydrophobicity of the monomer and the copolymers.

Keywords: Eugenol, benzoxazine, Co-polymer, Anti-corrosive coating and DFT.

INTRODUCTION

Corrosion means degradation of metal or alloys by direct interaction with the environment. Mild steel can widely use in large number of applications, marine application, pipelines which are highly used to transport oils and gases[1-3], open air structure[4], etc., So it is important to protect these metals and metal alloys from this destruction, many researchers developed new organic compounds as inhibitors[5-7], inorganic compounds[8-10], nano particles[11-13], plant extracts[14-18], even polymers as inhibitors due to their availability, inherent stability, low price and cost effective[19-21]. Among the polymers, recently polybenzoxazine which is known for molecular design flexibility, during curing process forming a thermosetting polymer without any catalyst, and it plays an important role in the corrosion inhibition due to its high thermal stability and small value of hydrophobicity, dielectric constant[22-26]. In order to minimize the health affect caused by the BPA monomer, now many researchers synthesized polybenzoxazine from bisguaicol-F[27], cardanol[28], sesamol[29],

curcumin[30], guaicol[31], eugenol[32,33], vanillin[34,35] etc., Polyurethanes are produced by the reaction of isocyanates with polyols or suitable catalyst, which are widely used in industrial purposes due to its, good chemical resistance, flexibility, adhesion, etc., it is widely used in the anti-corrosive agent[36,37] and bio-medical applications[38]. In order to explore more polymeric materials as a corrosion inhibitor, we have reported vanillin based benzoxazines that is copolymerized with polyurethane shown a very good anti-corrosive on mild steel in marine environment[39]. In that series, we have reported the synthesis and the corrosion resistance behaviour of the synthesized eugenol-based benzoxazine which is co-polymerized with polyurethane.

METHODS AND MATERIALS

Techniques applied

The IR spectrum was analyzed using a "Thermo Scientific Nicolet iS50 FT-IR Spectrometer", and the UV-spectrum was analyzed using a "Labman LMSP UV-1200 UV-Vis". "1H NMR" for the monomer observed on a "Bruker 500 MHz" with Dimethyl sulfoxide-D6 as a solvent. Also "13C NMR" for the same also recorded on a "Bruker 125 MHz" instrument. Thin Layer Chromatography (TLC) was observed to confirm the product formation. The surface is analysed using scanning electron microscope "JEOL JSM 6390" with 20 keV energy employed on the acceleration beam.
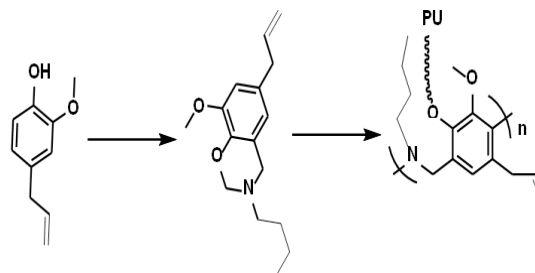
Synthesis of Monomer ("6-allyl-3-butyl-8-methoxy-3, 4-dihydro-2H-benzo[e][1,3] oxazine")

Paraformaldehyde (0.383 g, 12.789 mmol) and n-butylamine (0.601 mL, 6.090 mmol) were dissolved in chloroform (10 mL) and stirred at 50°C for 30 minutes. Then, euginol (0.943 mL, 6.090 mmol) and chloroform (20 mL) were added to the solution and stirred for 16 h at 70°C. TLC was used to check the progress of the reaction, and 100 mL of chloroform was added to the reaction mixture before filtering. The filtrate was then washed with water, brine solution, and 1N sodium hydroxide solution. It was separated from the organic material and dried over anhydrous sodium sulphate. The monomer was produced when the solvent evaporated.

Polymerization of the benzoxazine with isocyanate hardener on the mild steel

The synthesized monomer was dissolved

in 1,4-dioxane, to that solution isocyanate hardener in toluene was added. Benzoxazine was mixed with three different ratios of isocyanate hardener (100:60, 100:80, 100:100) were prepared. The emery paper was used polish the metal surface to improve the adhesion on mild steel plates and then the plates were cleaned by using water, hexane and acetone to remove impurities. The cleaned MS was then coated with BZ:PU solution using the dip-coating technique for 1 min, and then was slowly removed from it at a speed of 100 mm/minute. The coated MS was subsequently thermally dried and cured for three hours at 200°C in a furnace. The study by the EIS focused on coated mild steel.

Scheme 2. Synthesis of polyurethane-copolymerized monomer (6-allyl-3-butyl-8-methoxy-3, 4-dihydro-2H-benzo[e][1,3]oxazine)

Density Functional Theory computational studies

The computational calculations and representation of HOMO and LUMO using the Gaussian 09W program were studied using density functional theory. The B3LYP/6.31 G basis set was used to optimize the monomer's chemical structure. The Gauss view software package was used to visualize the computed structures of the HOMO, LUMO, and MEP (molecular electrostatic potential) representations.

Corrosion Studies by Tafel Polarization experiment and Electrochemical Impedance Spectroscopy (EIS) experiments

The Biologic SP 300 model machine was used for the polarization studies; it has three electrodes, with Ag/AgCl serving as the reference electrode and Pt serving as the counter electrode; efficiency of corrosion was calculated from I_{corr} value from Tafel extrapolation and the R_{ct} value obtained from the Nyquist plot.[31-39]

Studies on Water absorption

To analyze the hydrophobicity of the cured coated samples were done by ASTM D570 method,

which involved the immersion of monomer and copolymer coated and cured samples in water for 24 hours. The weight of the cured samples was noted before (Wa) the immersion. After 24 h, the water flecks are drained with a paper towel, removed. Then weight of the samples was noted (Wb). The percentage of absorption of the water particles were calculated by weight difference.[31-39]

Studies on Gel absorption

The entire investigation the weighing method was used to calculate the gel absorption of monomer and all the coated, cured copolymer sample. Before the investigation the weight of each sample was noted (Wb). After 24 h of immersion at RT, the samples were removed from the xylene an dried in an oven under vacuum, after this process the weight of all samples was again noted for (Wa). From the weight difference of the above two i.e., Wa and Wb the percentage of gel formation in the copolymer was calculated.[31,39]

RESULTS AND DISCUSSION

NMR spectrum of the synthesised Monomer from Eugenol

To confirm the structure of the monomer "1H NMR and 13C NMR" analysis was employed. The nine alkyl protons from the n-butylamine are appeared in the aliphatic region from 1.3ppm to 2.4ppm. five protons from allyl group attached to the eugenol ring appeared at the region 3.2, 5.1 and 5.8ppm. Two aromatic protons in the aromatic ring appeared in the region 6.4 and 6.5ppm (41, 42). Methoxy protons on the aromatic ring observed at the region 3.8ppm. The peaks appeared in the region 3.8 and 3.9ppm are respective for four protons from the benzoxazine ring which confirms the benzoxazine formation. Following the integration, 23 protons were accounted for Furthermore, 13C-NMR provides accurate details of monomer's structure. The alkyl chain carbon from n-butylamine shows their peaks at the aliphatic region 14.1, 20.4, 30.4 and 50ppm respectively. Similarly, the allyl carbons on the eugenol ring shows their chemical shift at 39.9, 137.7 and 115.5ppm. The peaks at the region 109.8, 122.5, 130.5, 138, 147.2 and 147.6ppm were responsible for the aromatic carbon moieties[41-43]. The methoxy carbon on the aromatic ring shows its chemical shift in 55.9ppm and the benzoxazine ring carbons chemical shift at the region 51.2 and 82.9ppm which also conforms the benzoxazine formation. From

NMR analysis the monomer structure shown in the Scheme 1 was confirmed.

Fig. 1a. 1H-NMR of the Benzoxazine monomer synthesised from eugenol

Fig. 1b. 13C NMR spectrum of the monomer synthesised from eugenol

IR spectrum of pure EuBz and blends with EuBz-PU

The "FT-IR spectra" of the monomer and all the copolymer with monomer and isocyanate hardener were shown in the Fig. 2. The symmetric and the asymmetric stretching of the -CH from the -CH$_2$ of the formed benzoxazine and the eugenol side chain appeared at 2946 and 2857 cm^{-1}. At higher wavenumber no stretching frequencies were observed which indicates that the heteroatom was devoid of any other labile protons, which ruled out the presence of 1° and 2° amine group, but the presence of 3° amine is confirmed. The asymmetric stretching frequency of -C-O- is represented at 1279 cm^{-1} band, while the symmetric stretching is represented by the band at 1227 cm^{-1}. The band at 925 cm^{-1} confirms the formation of a benzoxazine ring[41,45]. Other aromatic

-CH band appeared at 1504 cm^{-1} and the band at 3450 cm^{-1} represents the -N-H stretching frequency, which is present in the polyurethane attached to the polybenzoxazine. A peak at 1673 cm^{-1} corresponds to the carbonyl group from the benzoxazine monomer and this peak was strongly visible as a result of polyurethane incorporation into the our monomer.
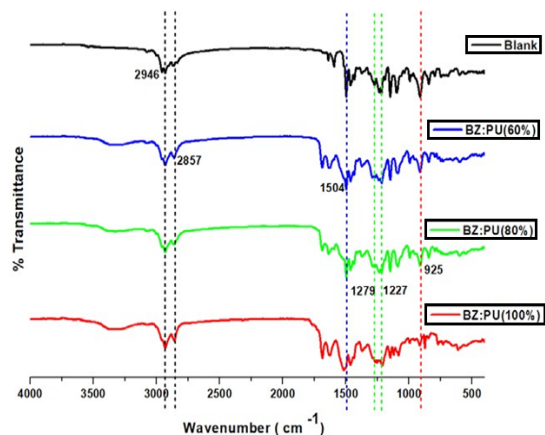

Fig. 2. FT-IR spectrum of polyurethane copolymers with eugenol-based monomers at various concentrations

VaBz monomer and VaBz-PU blends' UV-Vis spectrum

The monomer exhibits bands weak 250nm and 284nm which are attributed to the π-π^* electronic transition. The isocyanate loaded eugenol based benzoxazine shows two peaks at 269 and 282nm which are attributed to the π-π^* and n-π^* transition[46,47]. Observed an alteration in the π-π^* band during the copolymerization with isocyanate. The band that corresponds to the n-π^* transition also increased its absorbance, clearly demonstrating how significantly the isocyanate induced the monomer's electronic transition.
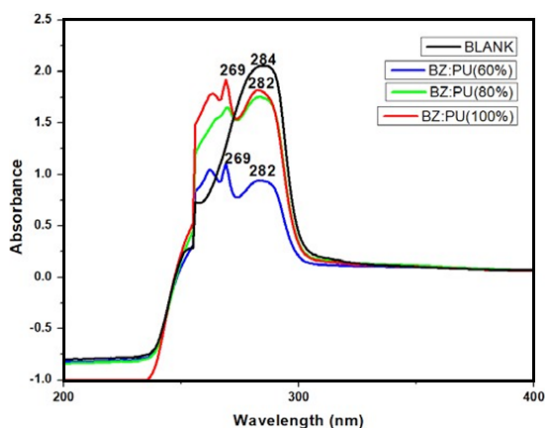
Fig. 3. UV spectrum of the eugenol-based monomer and its copolymer with polyurethane in different concentration

Corrosion Studies
Electrochemical studies by "Potentiostatic Polarization"

The Tafel polarization curves for the coated and cured copolymers of benzoxazine from eugenol and urethane were shown in Fig. 4. The I_{corr} and E_{corr} values were calculated by "superimposing the straight line along a linear portion of the anodic or cathodic curve". In general, a high value corrosion current (I_{corr}) represents the destructive metal allows for frequent electron mobility, which leads the metal to corrode easily which in turns give them with large corrosion rate on its surface. On the other hand, more, positive value of corrosion potential (E_{corr}) represents less corrosion rate[48,49]. From this information, the Tafel data for the eugenol based benzoxazine and its copolymers with different concentration were tabulated in the Table 1. In which, the uncoated mild steel shows more I_{corr} value and negative E_{corr} value, hence it represents more corrosion took place on it. Whereas the mild steel coated and cured with eugenol based benzoxazine copolymerized with urethane improves the corrosion current and corrosion potential against destruction. The EuBz: 60% PU coated material attained I_{corr} and E_{corr} value of 4.61µA and 131mV respectively, this was enhanced by coating the mild steel with EuBZ: 80% PU, also which was enhanced by coating with EuBz: 100% PU. From which we evidently show that corrosion rate decreased with increasing with urethane content on the mild steel, because more urethane makes the benzoxazine to form an effective noble layer for metal surface by providing more crosslinking ability. 60% urethane coated shows 36.68% corrosion efficiency than the uncoated mild steel, 80% urethane coated shows 72.53% corrosion efficiency and 100% urethane coated mild steel shows 74.73% corrosion efficiency. We can infer from the free energy of adsorption that the polymeric substance's physisorption onto the metal surface prevented corrosion.

Electrochemical system behaviour of BZPU coatings

One of the best techniques for determining a material's resistivity is the EIS method. The EIS for our samples were recorded in 3.5% sodium chloride solution and data for the blank and the EuBz:60%PU, EuBz:80%PU and EuBz:100%PU coated and cured mild steel were shown in the Table 2. Fig. 5 depicts the Nyquist plot, which has two-timed constants that are represented by a depressed capacitive semicircle that is found at higher frequencies and an inductive loop that is found at lower frequencies.

Earlier corrosion constant is associated with respect to charge transfer, whereas later corrosion constant is associated with the discovery of an intermediate product produced by the corrosion. Using the values obtained, the charge transfer resistance (R_{ct}) of the coated and blank mild steel was used to calculate the corrosion efficiency. The R_{ct} value increases by increasing urethane content on the mild steel, here the 60% loaded mild steel does not show much progress whereas the other two specimens with 80% and 100% urethane shows good resistance against corrosion. The materials' electrochemical properties are explained by another element known as the capacitance of the double layer (C_{dl})[50,51]. Furthermore, to simulate the impedence behaviour of the electrical double layer, the constant phase element (CPE) is used in the model rather than the ideal electrical capacitance. According to Table 2, uncoated mild steel has the least value when compared to metal (mild steel) coated with EuBz:PU, and it is clear that 80% and 100% loaded urethane in the coating raises the C_{dl} value, due to a reduction in the thickness of the electrical double layer or a rise in the local dielectric constant near the metal surface.

(a)

(b)

(c)

(d)
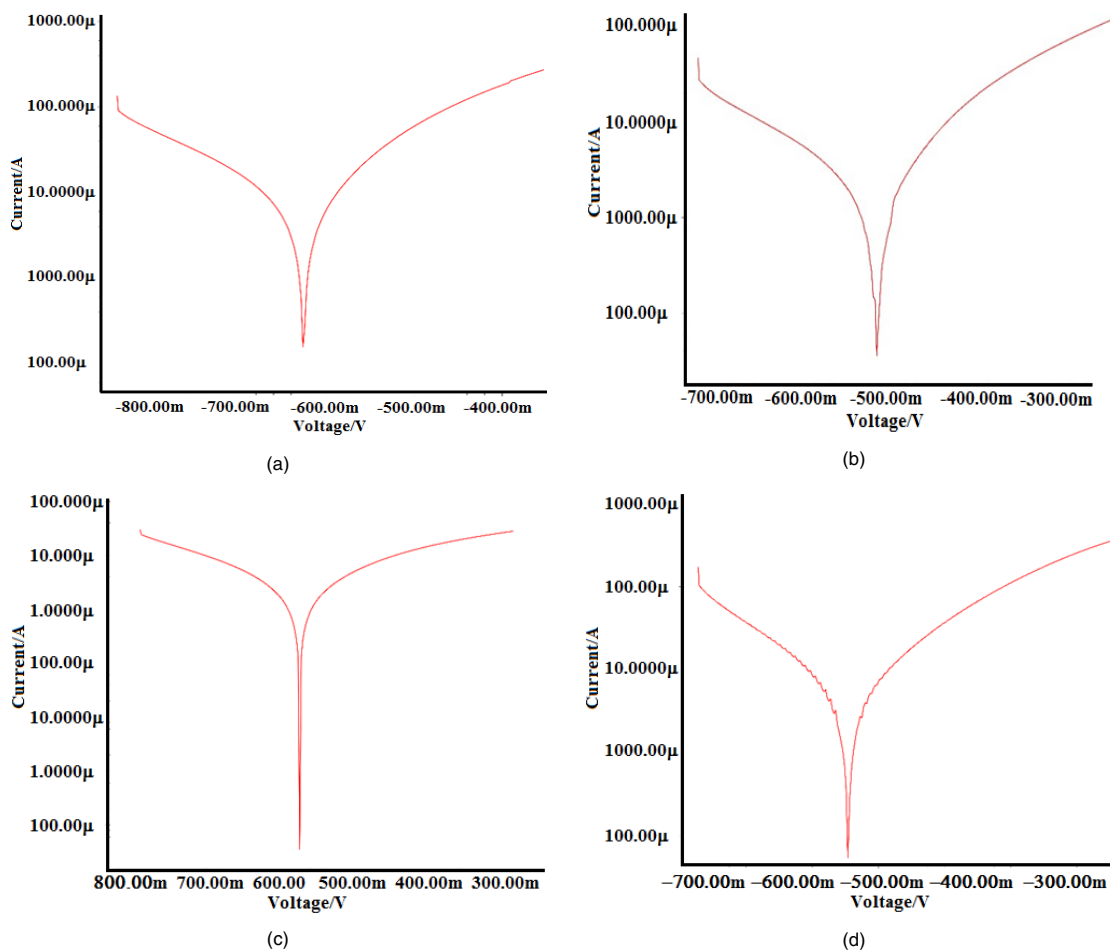
Fig. 4a. Tafel plot for the blank Mild steel, 4a, 4b and 4c-Tafel plots for the Mild steel with EuBZ:60%PU, EuBZ:80%PU and EuBZ:100%PU respectively

Table 1: Measurement derived from the Tafel experiment

	I_{corr}(µA)	E_{corr} (mV)	Rate of Corrosion (empty)	Coverage on the Metal Surface(θ)	Inhibition Efficiency (%)	Constant from the Tafel plots βa mV/dec	βcmV/dec	Free energy (ΔGads) KJ/mol
Blank 100:60	7.28	-638	84660	-	-	-179	159	-
(EuBZ:PU) 100:80	4.61	-621	53610	0.3668	36.68	-136	132	-9.88
(EuBZ: PU) 100:100	1.84	-518	21398	0.7473	74.73	-172	131	-12.66
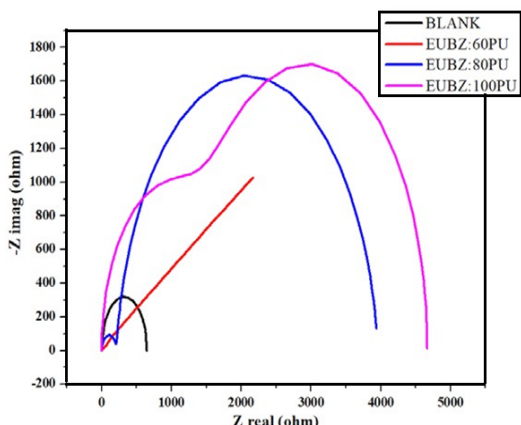
Fig. 5. Nyquist plot for the blank, EuBZ:60%PU, EuBZ:80%PU and EuBZ:100%PU coated Mild steel

Table 2: Results obtained from the Nyquist plot

Concentration of coating	R_{ct} Ω cm^2	C_{dl} F/cm^2	Corrosion Inhibition-Efficiency (%)
Mild steel with no coating	647	7.150 X10^{-9}	
100:60 (EuBZ:PU)	652	2.427X 10^{-6}	0.77
100:80 (EuBZ: PU)	3961	105 X10^{-6}	83.54
100:100 (EuBZ: PU)	4660	20.58 X 10^{-6} and 3.211 X10^{-6}	86.12

Scanning microscopic analysis

The surface morphology of mild steel was analyzed using SEM and energy-dispersive X-ray analysis (EDAX) before and after one week of immersion in 3.5% NaCl. Fig. 6's findings suggest that mild steel that has not been coated has a smooth surface that becomes affected by corrosion after being submerged in sodium chloride solution. This causes the surface area to look rough.[52,53] This corrosion of mild steel was reduced by the coating of the developed eugenol based benzoxazine which was copolymerized with urethane. In particular, by increasing the amount of polyurethane from EuBz100: PU60 to EuBz100: PU100, the corrosion was significantly reduced. In contrast to blank mild steel, mild steel coated with EuBz100: PU60 exhibits a polished surface after corrosion, and this can be enhanced by the sample with EuBz100:PU80. Additionally, it was enhanced by the mild steel's EuBz100:PU100 coating, which exhibits an even more polished surface than EuBz100:PU80. This could also be added to one more evidence for the better corrosion resistance arises by increasing polyurethane content on the mild steel. This was also proven

from the EDAX analysis were shown in the Fig. 7. From it, is clear that the addition of polyurethane to the surface reduced the percentage of iron destruction after the exposure to the 3.5% NaCl.
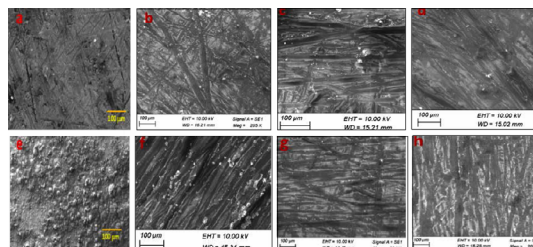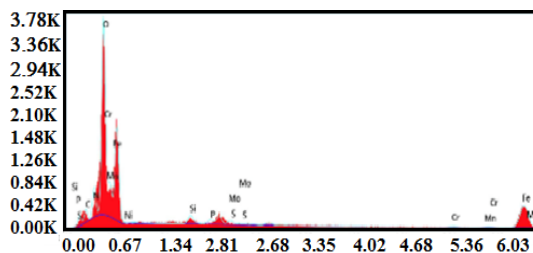

Fig. 6. SEM Pictures of the Blank and coated samples were employed "before immersion" (a to d) and "after immersion of 3.5% NaCl" (e to f), Uncoated mild steel (for a and d) EuBz: 60%PU (for b and f), 80%PU (for c and g), and 100%PU (for d and h)
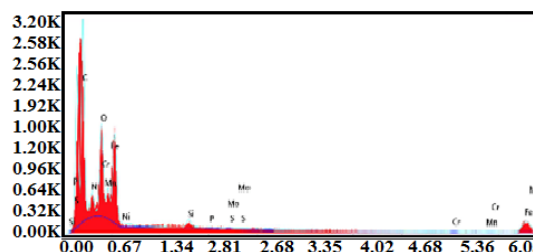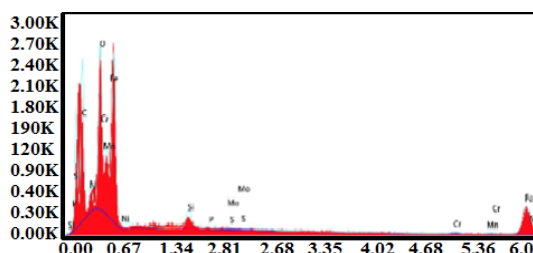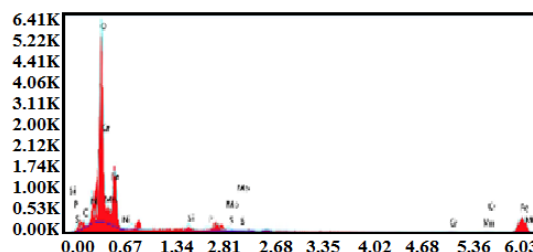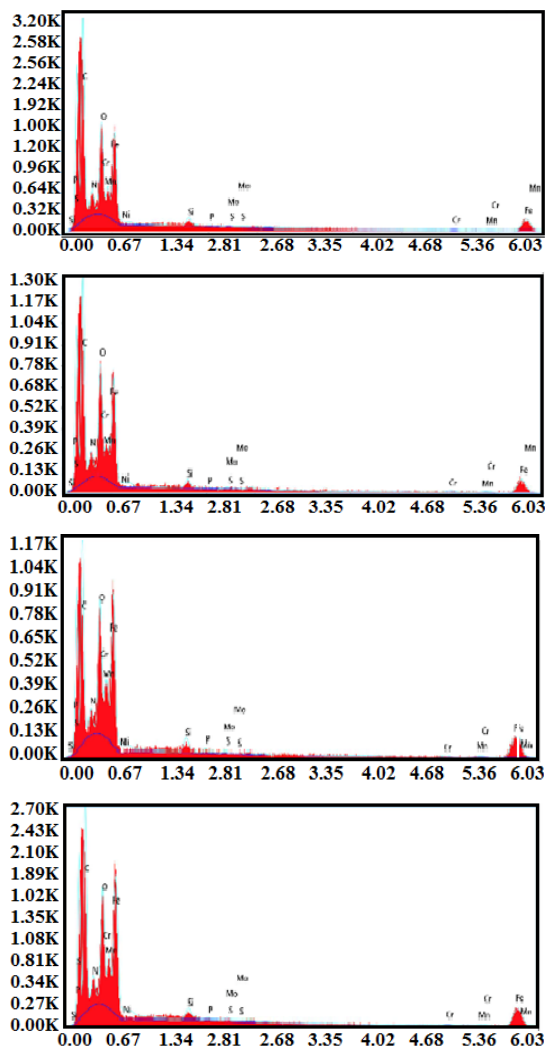
Fig. 7. Results from EDAX-Blank and coated samples were employed "before immersion" (a to d) and "after immersion of 3.5% NaCl" (e to f), Uncoated mild steel (a and d) EuBz: 60%PU (b and f), 80%PU (c and g), and 100%PU (d and h)

Water adsorption studies

The Hydrophobic character of the polymer materials plays a key role in the anti-corrosive property which was influenced by the branching, cross-linking ability of the material. The addition of coating agents like urethane, which resulted in the cross-linking property through hydrogen bonding, also had an impact on this hydrophobic property. It is evident that, the Fig. 8 shows that the increase in the polyurethane content on the coating shows much lesser water absorption property. The percentage of water absorption in the eugenol based benzoxazine was about 1.98%, this was reduced by 1.12% on mild steel

by adding 60% polyurethane, again it was reduced by 0.95% by adding 80% polyurethane, furthermore, reduced by 0.81% by the addition equal amount of benzoxazine with polyurethane (100% PU). From this study, it was concluded that the eugenol based benzoxazine with n-butylamine with urethane has significantly contributes towards the improvement of water absorption property, thereby we can say this polymer with urethane can acts as a better corrosion protecting coating on the mild steel surface.
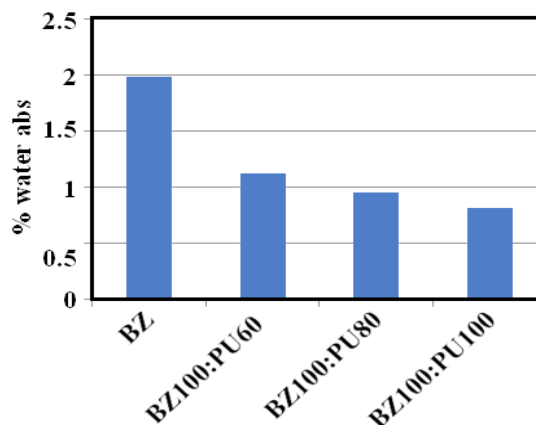
Fig. 8. Water absorption experiment results for the Mild steel coated with eugenol based benzoxazine and its copolymers with 60%, 80% and 100% polyurethane
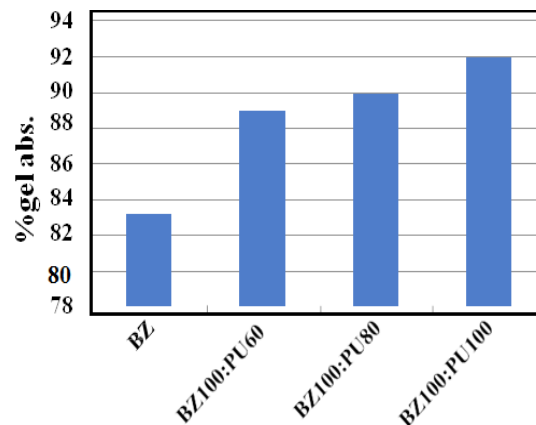

Fig. 9. Gel absorption experiment results for the Mild steel coated with eugenol based benzoxazine and its copolymers with 60%, 80% and 100% polyuretha

Gel absorption studies

In order to understand the polymer's ability to form stronger intra-linkages with one another, gel absorption studies are also crucial. This reduces the material's porosity, which in turn lessens water diffusion into it. So, the monomer and its polymers with copolymers were examined for this study. From

Fig. 9, monomer alone shows its gel formation with xylene by 83.15%, which was increased by 88.98% with the addition of 60% PU, which was further increased by 90.06% upon adding 80% PU and finally it was increased 92.11% with equal amount of monomer and urethane (100% PU). We can infer that the benzoxazine and polyurethane can act as a better anticorrosive coating on the mild steel surface based on the results of the improved gel absorption.

Quantum Chemical Calculations 3.8a-DFT analysis

The quantum chemical descriptors, such as HOMO, LUMO, band gap (ΔE), chemical potential, the global hardness (η), the global softness (θ), the electrophilicity index of the eugenol based benzoxazine monomer and its polymerization with hexamethylene isocyanate are shown in the Table 3. The HOMO is frequently linked to a molecule's capacity to donate electrons. A molecule's propensity to donate electrons to a suitable molecule with a low energy or partially filled molecular orbital is higher if it has a higher HOMO value. Therefore, if a molecule has a higher HOMO value, it will have a greater tendency to donate electrons to the metal's surface, leading to the highest adsorption and the greatest inhibition efficiency. In our experiment shows the EHOMO of EuBZ: PU has greater value than EHOMO of EuBZ, which clearly explains that the polyurethane loaded material shows better inhibition efficiency.[54]

Table 3: DFT Studies parameters

Compound	EHOMO(eV)	ELUMO(eV)	ΔE(Band gap) (eV)	Chemical Potential	Global Hardness(η)	Global Softness(σ)	Electrophilicity Index(ω)
EuBZ	-5.4195	-0.1877	5.2317	-2.8036	2.6158	0.1911	1.5024
EuBz-Urethane	-2.1826	-0.3028	1.879	-1.2427	0.9399	0.5319	0.8216
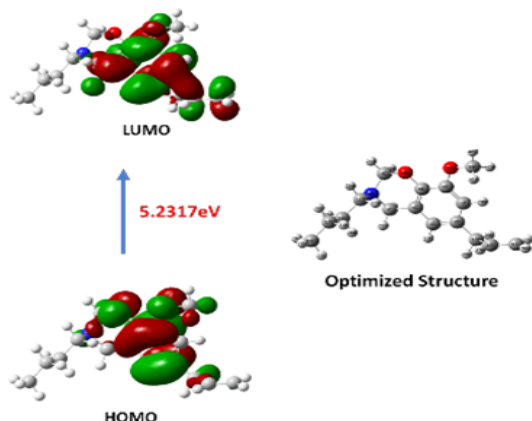
Fig. 10. FMO analysis of the benzoxazine monomer based on eugenol and its improved structure

Fig. 11. FMO analysis of eugenol based benzoxazine monomer and its optimized structure along with urethane

A molecule with a large band gap (ΔE) is more stable and associated with low reactivity, while a molecule with a small band gap (ΔE) is highly reactive, easily polarized, and can thus be readily adsorbed on the surface of a metal. As a result, the efficiency of this type of molecule is high. The value of global hardness (η) and softness (θ) can also be used to obtain information about molecular reactivity and selectivity. The HSAB concept serves as the foundation for the relationship between quantum chemical quantities and corrosion inhibition effectiveness.
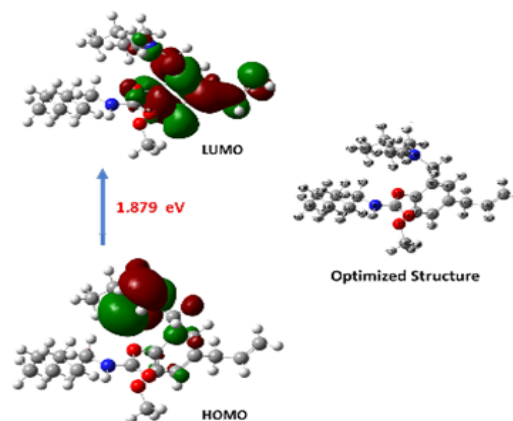
If an inhibitor has large value of hardness or small value of softness are being considered as a hard inhibitor. Similarly, an inhibitor has small value of global hardness and larger value of softness is being considered as soft molecule[55] therefore it can easily offer electron density to the acceptor which makes them highly reactive than the hard inhibitor molecule. Also, adsorption on the metal surface can be easy when an inhibitor has highest softness value. In that aspect also, EuBZ:PU (0.5319)> EuBz (0.1911) monomer, which evidently conclude that the urethane loaded benzoxazine become a good inhibitor than the benzoxazine monomer. According to definitions, electrophilicity refers to a

chemical species' reactivity in attracting electrons from its nucleophile. The opposite of electrophilicity is called nucleophilicity (ε).If an inhibitor molecule having larger electrophilicity value are considered as ineffective towards corrosion inhibition, hence a molecule with small electrophilicity or large nucleophilicity can acts as a good inhibitor[56] In that aspect also our experiment shows that EuBZ:PU (0.8216)>EuBz(1.5024) monomer, we confirmed the urethane loaded benzoxazine could acts as a better inhibitor than the monomer.

Molecular electrostatic potential (MEP)

The quantum chemical method can also be used to calculate a molecule's chemical reactivity by displaying the electron distribution on the molecule as a coloured map[54]. The color served to distinguish between compounds with optimized structures for positive, negative, and neutral electrostatic potential. More negative potential in a molecule can be indicated by the colour red, moderate negative potential by the colour yellow, and more positive potential by the colour green. The molecule's neutral or zero electron potential is represented by the colour blue. From the above Fig. 12 and Fig. 13, it is clear that the red colour is obtained around the oxygen atoms present in the molecule and yellow region around the nitrogen in the molecule which in turn represents the negative potential region that able to adsorbed on the metal surface. The allyl and the butyl group represents green colour that is the positive potential region. The blue region observed in the hexyl unit of the urethane in the urethane loaded copolymer in Figure 13.
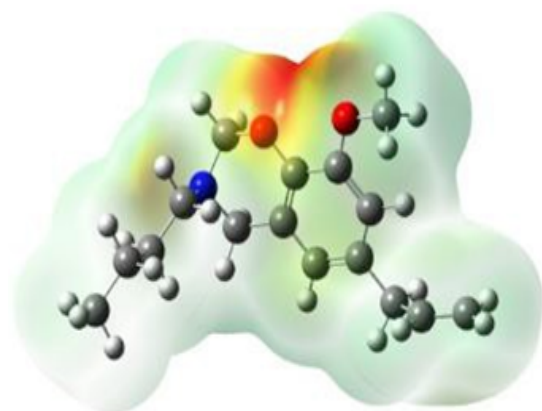

Figure 12: Molecular electrostatic potentialmapping of the eugenol based benzoxazine
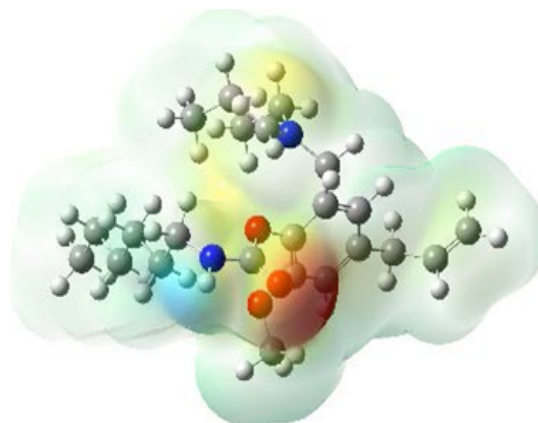

Fig. 13. Molecular electrostatic potential mapping of the eugenol based benzoxazine along with urethane

CONCLUSION

With the help of n-butylamine, paraformaldehyde, and eugenol, we were able to successfully synthesize benzoxazine, which was then thoroughly characterized using UV-Visible spectroscopy, NMR, and FT-IR. It was determined after studying the anti-corrosive properties of monomers with copolymers that were 60%, 80%, and 100% urethane loaded that the urethane addition improved corrosion inhibition on mild steel. The combination of 100% urethane coating and benzoxazine exhibits the best overall corrosion inhibition. Studies on water and gel absorption provided additional support for the hydrophobic behaviour of the monomer and its copolymers, confirming that polyurethane with a 100% urethane content is hydrophobic and serves as an excellent anti-corrosive coating on the surface of mild steel. The results of surface morphological studies from SEM, elemental analysis EDAX, and theoretical studies DFT support our work toward the anti-corrosive property of the monomer and its copolymers.

ACKNOWLEDGMENT

Conflict of interests

Authors declare that no conflict of interest.

REFERENCES

1. Idelfitri, N. I. F.; Dzulkifli, N. N.; Ash'ari, N. A. N.; Sapari, S.; Razak, F. I. A.; Pungot, N. H. *Inorg. Chem. Commun.*, **2023**, *150*, 110485; https://doi.org/10.1016/j.inoche.2023.110485.

2. Ikpeseni, S. C.; Owamah, H. I.; Owebor, K. *J Bio Tribo Corros.*, **2021**, *7*, 84;https://doi.org/10.1007/s40735-021-00505-8

3. Barbouchi, M.; Benzidia, B.; Aouidate, A.; Ghaleb, A.; El Idrissi, M.; Choukrad, M. *J. King Saud Univ. Sci.*, **2020**, *32*(7), 2995-3004; https://doi.org/10.1016/j.jksus.2020.08.004

4. de la Fuente, D.; Díaz, I.; Simancas, J.; Chico, B.; Morcillo, M. *Corros. Sci.*, **2011**, *53*(2), 604-617; https://doi.org/10.1016/j.corsci.2010.10.007

5. Bahrami, M.J.; Hosseini, S.M.A.; Pilvar, P. *Corros. Sci.*, **2010**, *52*, 9, 2793-2803; https://doi.org/10.1016/j.corsci.2010.04.024

6. Carranza, M. S. S.; Reyes, Y. I. A.; Gonzales, E. C.; Arcon, D.P.; Franco, F. C.; *Heliyon.*, **2021**, *7*, 9;https://doi.org/10.1016/j.heliyon.2021.e07952

7. Chen, L.; Lu, D.; Zhang, Y. *Materials.,* **2022**, *15*(6), 2023; https://doi.org/10.3390/ma15062023

8. Baach, B.; Ouakki, M.; Ferraa, S.; Barebita, H.; Cherkaoui, M.; Nimour, A.; Guedira, T. *Inorg. Chem. Commun.*, **2022**, *137*, 109233; https://doi.org/10.1016/j.inoche.2022.109233

9. Deyab, M.A.; Eddahaoui, K.; Essehli, R.; Rhadfi, T.; Benmokhtar, S.; Mele, G.; *Desalination.*, **2016**, *383*, 38-45; https://doi.org/10.1016/j.desal.2016.01.019.

10. Ramezanzadeh, M.; Bahlakeh, G.; Ramezanzadeh, B. *J. Mol. Liq.*, **2019**, *292*, 111387; https://doi.org/10.1016/j.molliq.2019.111387.

11. Fedel, M.; Ahniyaz, A.; Ecco L.G.; Deflorian, F. *Electrochim. Acta.*, **2014**, *131*, 71-78; https://doi.org/10.1016/j.electacta.2013.11.164.

12. Sharmila, R.; Selvakumar, N.; Jeyasubramanian, K. *Mater. Lett.*, **2013**, *91*, 78-80; https://doi.org/10.1016/j.matlet.2012.09.051

13. Narenkumar, J.; Parthipan, P.; Madhavan, J.; Murugan, K; Marpu, S.B.; Suresh, A. K. *Environ. Sci. Pollut. Res.*, **2018**, *25*, 5412-5420; https://doi.org/10.1007/s11356-017-0768-6

14. Al-Otaibi, M.S.; Al-Mayouf, A.M.; Khan, M.; Mousa, A.A; Al-Mazroa, S.A.; Alkhathlan, H.Z. *Arab. J. Chem.*, **2014**, *7*(3), 340-346; https://doi.org/10.1016/j.arabjc.2012.01.015

15. Uwah, I. E.; Okafor, P. C.; Ebiekpe, V. E. *Arab. J. Chem.*, **2013**, *6*(3), 285-293;https://doi.org/10.1016/j.arabjc.2010.10.008

16. Prabakaran, M.; Hyun Kim, S.; Kalaiselvi, K.; Hemapriya, V.; Min Chung, *J. Taiwan Inst. Chem. Eng.*, **2016**, *59*, 553-562; https://doi.org/10.1016/j.jtice.2015.08.023

17. Umoren, S.A.; Obot, I.B.; Israel, A.U.; Asuquo, P.O; Solomon, M.M.; Eduok, U.M.; Udoh, A.P. *J. Ind. Eng. Chem.*, **2014**, *20*(5), 3612-3622;https://doi.org/10.1016/j.jiec.2013.12.056

18. Uwah, I.E.; Okafor, P.C.; Ebiekpe, V.E. *Arab. J. Chem.*, **2013**, *6*(3), 285-293; https://doi.org/10.1016/j.arabjc.2010.10.008

19. Azzam, M.S.; Abd El-Salam, M.; Mohamed, A.; Shaban, M.; Shokry, A. *Egypt. J. Pet.*, **2018**, *27*(4), 897-910; https://doi.org/10.1016/j.ejpe.2018.01.006

20. Umoren, S.A.; Ogbobe, O.; Igwe, I.O.; Ebenso, E.E. *Corros. Sci.*, **2008**, *50*(7), 1998-2006; https://doi.org/10.1016/j.corsci.2008.04.015.

21. Ocón, P.; Cristobal, A.B;. Herrasti, P.; Fatas, E. *Corros. Sci.*, **2005**, *47*(3), 649-662 (2005); https://doi.org/10.1016/j.corsci.2004.07.005.

22. Ishida, H. Allen, D. J. *J. Polym. Sci. B Polym. Phys.*, **1996**, *34*, 1019. https://doi.org/10.1002/(SICI)1099-0488(19960430)34:6<1019::AID-POLB1>3.0.CO;2-T

23. Liu, J.; Lu, X.; Xin, Z.; Zhou, C.L. *Langmuir.*, **2011**, *27*(13), 8365-8370, https://doi.org/10.1021/la200073v

24. Wang, L.; Yuan, M.; Zhao, Y.; Guo, Z.; Lu, X.; Xin, Z. *Prog. Org. Coat.*, **2022**, *167*, 106863 (2022); https://doi.org/10.1016/j.porgcoat.2022.106863

25. Mydeen, K. M.; Kanth, J.P.; Hariharan, A.; Krishanasamy, B.; Rameshkumar, S.; Radhiga, G.; Muthukaruppan, A. *J. Polym. Environ.*, **2022**, *30*, 5301–5312 https://doi.org/10.1007/s10924-022-02593-0

26. Ghosh, N.N; Kiskan, B; Yagci, Y. *Prog. Polym. Sci.*, **2007**, *32*(11), 1344-1391 https://doi.org/10.1016/j.progpolymsci.2007.07.002.

27. Thirukumaran, P.; Shakila Parveen, A.; Kumudha, K.; Sarojadevi, M.; Kim, S.M. *New J. Chem.*, **2016**, *40*, 9313-9319 https://doi.org/10.1039/C6NJ02242A

28. Ranganathan, S.; Arumugam, H.; Krishnasamy, B.; Sathy Srikandan, S.; Mallaiya, K.; Alagar, M. High Perform. *Polym.*, **2022**, *34*(5), 593-603 https://doi.org/10.1177/09540083221085163

29. Liu, X.; Li, Z.; Zhan, G.; Wu, Y.; Zhuan, Q. *J. Appl. Polym. Sci.*, **2019**, *136*(48), 48255 https://doi.org/10.1002/app.48255

30. Deng, Y.; Xia, L.; Song, G. L.; Zhao, Y.; Zhang, Y.; Xu, Y.; Zheng, D *Compos. B Eng.*, **2021**, *225*, 109263 https://doi.org/10.1016/j.compositesb.2021.109263.

31. Ganesh Phalak, A.; Deepak Patil, M.; Mhaske, S.T. *Eur. Polym. J.*, **2017**, *88*, 93-108 https://doi.org/10.1016/j.eurpolymj.2016.12.030

32. Chen, C; Cao, Y; Lu, X; Li, X; Yao, H; Xin, Z. *Colloids Surf. A: Physicochem. Eng.*, **2021**, *609*, 125605 https://doi.org/10.1016/j.colsurfa.2020.125605

33. Mahajan, M. S.; Mahulikar, P. P; Gite, V. V. *Prog. Org. Coat.*, **2020**, *148*, 105826 https://doi.org/10.1016/j.porgcoat.2020.105826

34. Soudjrari, S.; Derradji, M.; Amri, B.; Khawla, D.; Sana, T.; Noureddine, R.; Wenbin, L.; Azzedine, K. *High Perform. Polym.*, **2022**, *34(7*), 818-827 https://doi.org/10.1177/09540083221088738

35. Sini, N. K.; Jayashree, B.; Varma, I. K. *Polym. Degrad. Stab.*, **2014**, *109*, 270-277 https://doi.org/10.1016/j.polymdegradstab.2014.07.015.

36. Tong, Y; Bohm, S; Song, M. *Appl. Surf. Sci.*, **2017**, *424*(1), 72-81https://doi.org/10.1016/j.apsusc.2017.02.081

37. González-García, Y; González, S; Souto, R. M. *Corros. Sci.*, **2007**, *49*(9), 3514-3526https://doi.org/10.1016/j.corsci.2007.03.018

38. Joseph, J.; Patel, R.M.; Wenham, A.; Smith, J. R. *Inst. Met. Finish.*, **2018**, *96*(*3*), 121-129 https://doi.org/10.1080/00202967.2018.1450209.

39. Jayanthi, K.; Sivaraju, M.; Shanmugasundaram, P. *Asian J. Chem.*, **2023**, *35*(4), 851-860 https://doi.org/10.14233/ajchem.2023.27290.

40. Velrani, S; Jeyaprabha, B; Prakash, P. *Int. J. Innov. Sci. Eng. Technol.*, **2014**, *1*(10), 57-69.

41. Thirukumaran, P.; Shakila, A.; Muthusamy, S. *RSC Adv.*, **2014**, *4*, 7959-7966 https://doi.org/10.1039/C3RA46582A

42. Thirukumaran, P.; Shakila Parveen, A.; Sarojadevi, M. *ACS Sustain. Chem. Eng.*, **2014**, *2*(12), 2790-2801 https://doi.org/10.1021/sc500548c

43. Vikashini, R.; Arumugam, H.; Krishnasamy, B.; Latha, G.; Subbian, M.; Alagar, M. *Polym-Plast. Techn. Mat.*, **2022**, *61*(4), 415-425, 10.1080/25740881.2021.1991951

44. Li, W.; Xiao, L.; Wang, Y.; Chen, J.; Nie, X. *Polymer.*, **2021**, *229*, 123967 https://doi.org/10.1016/j.polymer.2021.123967

45. Hussein, M. M.; Saafan, S. A.; Salahuddin, N. A.; Omar, M. K. *Applied Physics A*, **2021**, *127*, 488 https://doi.org/10.1007/s00339-021-04620-8

46. Kumar, N.; Yadav, N.; Amarnath, N.; Sharma, V.; Shukla, S.; Srivastava, A.; Prasad, P.; Kumar, A.; Swati, G.; Shailja, S.; Seema, S.; Bimlesh, L. *Mo.l Cell Biochem.*, **2019**, *454*, 123–138 https://doi.org/10.1007/s11010-018-3458-x

47. Chowdaiah, M.; Sharma, P.; Dhamodhar, P.; *In.t J. Pept. Res. Ther.*, **2019**, *25*, 1581–1593 https://doi.org/10.1007/s10989-018-09801-3

48. Mirzakhanzadeh, Z; Kosari, A; Moayed, M.H; Naderi, R; Taheri, P*. Corros. Sci.*, **2010**, *138*, 372-379 https://doi.org/10.1016/j.corsci.2018.04.040

49. Mobin, M.; Aslam, R. *Process Saf. Environ. Prot.*, **2018**, *114*, 279-295 https://doi.org/10.1016/j.psep.2018.01.001

50. Sanaei, Z.; Shahrabi, T.; Ramezanzadeh, B. *Dyes Pigm.*, **2017**, *139*, 218-232. https://doi.org/10.1016/j.dyepig.2016.12.002

51. Dinesh Kumar, G.; Prabunathan, P.; Manoj, M.; Hariharan, A.; Alagar, M *J. Polym. Environ.*, **2020**, *28*, 2444–2456 https://doi.org/10.1007/s10924-020-01782-z

52. Tan, B.; He, J.; Zhang, S.; Xu, C; Chen, S.; Liu, H.; Li, W. *J. Colloid Interface Sci.*, **2020**, *585*, 287-301 https://doi.org/10.1016/j.jcis.2020.11.059

53. Vorobyova, V.; Skiba, M. *Waste Biomass Valor.*, **2021**, *12*, 4623–4641 https://doi.org/10.1007/s12649-020-01333-6

54. Kadhim, A.; Al-Okbi, A.K.; Jamil, D.M.; Qussay, A.; Al-Amiery, A.A.; Gaaz, T.S.; Kadhum, A. A. H.; Bakar Mohamad, A.; Nassir, M.H. *Results Phys.*, **2017**, *7*, 4013-4019 https://doi.org/10.1016/j.rinp.2017.10.027

55. Sasikumar, Y.; Adekunle, A.S.; Olasunkanmi, L.O.; Bahadur, I.; Baskar, R.; Kabanda, M. M.; Obot, I. B.; Ebenso, E. E. *J. Mol. Liq.*, **2015**, *211*, 105-118 https://doi.org/10.1016/j.molliq.2015.06.052.

56. Kaya, S.; Tüzün, B.; Kaya, C.; Bassey Obot, I. *J. Taiwan Inst. Chem. Eng.*, **2016**, *58*, 528-535 https://doi.org/10.1016/j.jtice.2015.06.009.